

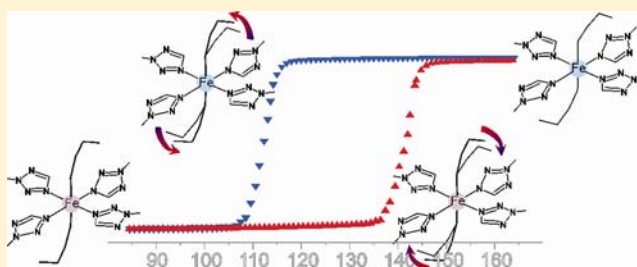
Role of Fe–N–C Geometry Flip-Flop in Bistability in Fe(tetrazol-2-yl)₄(C₂H₅CN)₂-Type Core Based Coordination Network

Agata Białońska and Robert Bronisz*

Faculty of Chemistry, University of Wrocław, F. Joliot-Curie 14, 50-383 Wrocław, Poland

Supporting Information

ABSTRACT: [Fe(ebtz)₂(C₂H₅CN)₂](ClO₄)₂ was prepared in the reaction of 1,2-di(tetrazol-2-yl)ethane (ebt) with Fe(ClO₄)₂·6H₂O in propionitrile. The compound crystallizes as a one-dimensional (1D) network, where bridging of neighboring iron(II) ions by two ebt ligand molecules results in formation of a [Fe(ebtz)₂]_∞ polymeric skeleton. The 1D chains are assembled into supramolecular layers with axially coordinated nitrile molecules directed outward. The complex in the high spin (HS) form reveals a very rare feature, namely, a bent geometry of the Fe–N–C(propionitrile) fragment (149.1(3)° at 250 K). The HS to low spin (LS) HS→LS transition triggers reorientation of the propionitrile molecule resulting in accommodation of a typical linear geometry of the Fe–N–C(nitrile) fragment. The switching of the propionitrile molecule orientation in relation to the coordination octahedron is associated with increase of the distance between the supramolecular layers. When the crystal is in the LS phase, raising the temperature does not cause reduction of the distance between supramolecular layers, which contributes to further stabilization of the more linear geometry of Fe–N–C(C₂H₅) and the LS form of the complex. Thus, a combination of Fe–N–C(C₂H₅) geometry lability and lattice effects contributes to the appearance of hysteretic behavior ($T_{1/2}^{\downarrow} \approx 112$ K, $T_{1/2}^{\uparrow} \approx 141$ K).



INTRODUCTION

One of the most interesting phenomena, the thermal induced spin crossover (SCO), arises from an ability of the transition metal octahedral complexes with 3d⁴–3d⁷ configuration to adopt two different electronic states.¹ In iron(II) complexes, the high spin (HS) to low spin (LS) HS(*S* = 2) ⇌ LS(*S* = 0) transition triggered by a change of temperature, an application of pressure,² magnetic field,³ or by light irradiation⁴ involves severe alterations of magnetic, optical, and dielectric⁵ properties which are the basis of potential applications.⁶ For practical applications, SCO materials have to exhibit an abrupt spin transition with a wide loop of hysteresis.⁷ According to the model of elastic interactions developed by Spiering,^{8,9} a perturbation produced by shortening of the Fe–N bond length involves a compression of a crystal lattice contributing additionally to a stabilization of the LS form of iron(II). It is assumed that in molecular systems, the cooperative nature of the SCO stems from a presence of intermolecular interactions¹⁰ enhancing a perturbation transmission on the adjusted SCO centers as well as on the whole crystal lattice. The interplay between short and long-range elastic interactions may lead to long-range ordering and superstructure formation in the intermediate phase accompanied by incomplete¹¹ or two step spin transitions.^{12,13} Unfortunately, a control of crystal packing in molecular systems is practically impossible. A polymeric approach, using a single dominating interaction between ligand and metal ion, depends on the connection of SCO centers by a system of the covalent bonded bridging ligands.^{14,15} In such a

case, a complementarity of building blocks, in term of their ability to form the coordination bonds, plays a predominant role in a self-assembly process.¹⁶ This approach gives a possibility to construct polymeric materials comprising a small number of unequivocally defined linkages between metal centers. Noteworthy, a careful design of ligand structure allows deliberate preparation of coordination networks; however, in most cases rational control of dimensionality and topology of the network is very limited.

Bis-^{17–22} and tris(tetrazol-1-yl)-type²³ ligands attract much attention because they are prone to form coordination networks, and analogously to complexes based on monodentate 1-substituted tetrazoles,²⁴ their iron(II) complexes exhibit the SCO phenomenon. Also bidentate ligands comprising 1,2,3-triazol-1-yl donors were successfully applied for construction of SCO coordination networks.²⁵ A review summarizing azole based complexes up to 2010 was performed by Aromi et. al.²⁶ Nevertheless, among the SCO polymeric materials, there are known complexes exhibiting abrupt as well as gradual SCO. Evidently an establishing of a direct linkage between SCO centers is not a sole and a sufficient condition for an occurrence of the cooperative spin transition. It is supposed that weakening of the elastic interactions may stem from a flexibility of the ligand molecules¹⁸ or an elasticity of the whole coordination network.^{15,27} An absence of strong intermolecular interactions

Received: April 30, 2012

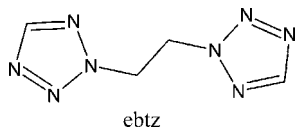
Published: November 14, 2012

between polymeric units are also pointed to as responsible for low cooperativity of the SCO.²⁸

Investigations of coordination properties of 1, ω -di(tetrazol-2-yl)alkanes revealed that also ligands based on 2-substituted tetrazoles as donor groups form one-dimensional (1D), two-dimensional (2D), and three-dimensional (3D) coordination networks.^{29,30} Moreover, similarly to complexes of iron(II) with 1-substituted tetrazoles, systems containing exclusively tetrazol-2-yl donors exhibit the SCO phenomenon.³¹ [Fe(pbtz)₃](ClO₄)₂·2EtOH (pbtz = 1,3-ditetrazol-2-yl)propane shows gradual SCO, and analogously to complexes of 1-substituted tetrazoles, a first coordination sphere of iron(II) consists of six tetrazol-2-yl rings coordinated through exodentate nitrogen atoms N4. Nevertheless, further studies revealed that bis-(tetrazol-2-yl)alkanes can form iron(II) complexes containing a [Fe(tetrazol-2-yl)₄(CH₃CN)₂]-type core. Namely, 2-hydroxy-1-(tetrazol-1-yl)-3-(tetrazol-2-yl)propane³² and 1,6-di(tetrazol-2-yl)hexane (hbtz)³³ react with iron(II) perchlorate giving 1D and 2D networks, respectively, in which axial positions are occupied by acetonitrile molecules. The above mentioned heteroleptic complexes also show thermally induced SCO.

Continuing our studies on the application of azole-based flexible/elastic ligands suitable for construction of SCO materials, we have prepared a 1D coordination polymer in which iron(II) ions are bridged by 1,2-di(tetrazol-2-yl)ethane (ebtz, Chart 1).

Chart 1



The heteroleptic system [Fe(ebtz)₂(C₂H₅CN)₂](ClO₄)₂ exhibits an abrupt SCO accompanied by a hysteresis loop. It

was found that spin transition is associated with serious alteration of Fe–N–C(propionitrile) geometry. To determine the role of coordinated propionitrile molecule orientational lability on SCO behavior, single crystal X-ray diffraction studies of the HS and LS forms were performed.

EXPERIMENTAL SECTION

Materials and Methods. The 1,2-di(tetrazol-2-yl)ethane (ebtz)²⁹ was synthesized according to the procedures described previously. Iron(II) perchlorate hexahydrate purchased from Aldrich was used. Synthesis of the iron(II) complex was performed under nitrogen atmosphere using the standard Schlenk technique; a few crystals of ascorbic acid were added to the reaction mixture to prevent iron(II) oxidation.

Caution! Even though no problems were encountered, it is worth mentioning that complexes containing perchlorates and tetrazole derivatives are potentially explosive and should be synthesized in milligram scale and handled with care.

Infrared spectra was recorded with the Bruker IFS66 IR FTIR spectrometer in the range 400–4000 cm⁻¹ in nujol mulls. Elemental analyses for carbon, hydrogen, and nitrogen were performed on Perkin-Elmer 240C analyzer. Temperature measurements of the magnetic susceptibility were carried out with a Quantum Design SQUID magnetometer in the 5–300 K temperature range at scan rate 1 and 0.1 K/min under 1 T applied magnetic field. Magnetic data were corrected for the diamagnetic contributions, which were estimated from Pascal's constants.

Synthesis of [Fe(ebtz)₂(C₂H₅CN)₂](ClO₄)₂ (1). A solution of Fe(ClO₄)₂·6H₂O (0.15 mmol, 0.0544 g) in propionitrile (5.0 mL) was added to a solution of ebtz (0.3 mmol, 0.0498 g) in propionitrile (5.0 mL). The resultant clear solution was concentrated in the stream of nitrogen to a volume of about 8 mL and was left in the closed Schlenk flask for one month. Next, colorless crystals were filtered off, washed with 1 mL of propionitrile, and dried in the stream of nitrogen. Yield 84% (0.087 g). Anal. found: C, 24.3; H, 3.0; N, 36.3%. Calc. for FeC₁₆H₂₄N₂₀Cl₂O₈ (M_w = 697.19): C, 24.1; H, 3.2; N, 36.2%. IR (nujol): 3144(s), 3131(s), 3024(m), 2955(s, sh), 2925(s), 2854(s), 2296(w), 2277(m), 1466(s), 1448(m, sh), 1416(w), 1389(s), 1377(s), 1353(w), 1323(w), 1303(s), 1210(m), 1196(m), 1186(s), 1157(s, sh),

Table 1. Crystallographic Data for 1

	temperature/K							
	250(2)	160(2)	110(2)	100(2) ^d	80(2)	110(2) ^c	120(2) ^c	160(2) ^c
chemical formula	C ₁₄ H ₂₂ Cl ₂ FeN ₁₈ O							
formula Mass	697.25							
crystal system	monoclinic							
space group	P21/n							
Z	2							
a/Å	8.388(2)	8.364(2)	8.354(2)	8.287(2)	8.144(2)	8.149(2)	8.168(2)	8.363(2)
b/Å	15.370(3)	15.170(3)	15.051(3)	15.054(3)	15.725(3)	15.727(3)	15.750(3)	15.172(3)
c/Å	11.616(3)	11.595(3)	11.587(3)	11.692(3)	11.217(3)	11.222(3)	11.242(3)	11.597(3)
α/deg	90.00	90.00	90.00	90.00	90.00	90.00	90.00	90.00
β/deg	106.75(3)	106.62(3)	106.54(3)	106.24(3)	107.64(3)	107.63(3)	107.64(3)	106.64(3)
γ/deg	90.00	90.00	90.00	90.00	90.00	90.00	90.00	90.00
unit cell volume/Å ³	1434.0(6)	1409.7(6)	1396.6(6)	1400.4(6)	1369.0(6)	1370.7(6)	1378.2(6)	1409.8(6)
absorption coefficient, μ/mm ⁻¹	0.786	0.799	0.807	0.805	0.823	0.822	0.817	0.799
no. of reflections measured	9589	9451	9327	8232	8994	9015	9080	9178
no. of independent reflections	3087	3036	3009	3041	2936	2943	2961	3032
R _{int}	0.0472	0.0443	0.0407	0.0532	0.0489	0.0557	0.0508	0.0594
final R ₁ values (I > 2σ(I))	0.0354	0.0349	0.0324	0.0350	0.0379	0.0399	0.0377	0.0394
final wR(F ²) values (I > 2σ(I))	0.0752	0.0756	0.0739	0.0950	0.0800	0.0746	0.0754	0.0692
final R ₁ values (all data) ^a	0.0714	0.0639	0.0561	0.0369	0.0747	0.0864	0.0773	0.0972
final wR(F ²) values (all data) ^b	0.0840	0.0823	0.0799	0.0963	0.0887	0.0841	0.0848	0.0812

^aR₁ = ∑||F_o| - |F_c|| / ∑|F_o|. ^bwR² = [∑w(F_o² - F_c²)² / ∑w(F_o²)²]^{1/2}. ^cHeating mode. ^dFast cooling.

1184(s), 1109(s, sh), 1090(s), 1075(s, sh), 1056(s), 1043(s), 1027(s), 1015(m), 960(w), 940(w), 924(w), 910(w), 785(w), 712(w), 701(s), 679(m), 658(m), 623(s), 654(w), 503(m) cm^{-1} .

X-ray Data Collection and Structure Determination. Crystals of **1**, obtained according with the aforementioned synthesis procedure, were coated by a layer of inert oil, and a suitable crystal was immediately transferred to the stream of gaseous nitrogen of the diffractometer ($T = 250$ K). Crystal structures at 250, 160, 110, and 80 K in cooling mode and at 110, 120, and 160 K in heating mode were determined. Crystal structure at 100 K was determined after fast cooling (2 K/min) from 110 K. Crystal data and refinement details are listed in Table 1. Measurements were performed using Oxford Cryosystem device on Kuma KM4CCD κ -axis diffractometer with graphite-monochromated $\text{MoK}\alpha$ radiation. The data were corrected for Lorentz and polarization effects. Analytical absorption correction was applied. Data reduction and analysis were carried out with the Oxford Diffraction (Poland) Sp. z o.o. (formerly Kuma Diffraction Wrocław, Poland) programs. The structures were solved by direct methods (program SHELXS97³⁴) and refined by the full-matrix least-squares method on all F^2 data using the SHELXL97³⁴ program.

RESULTS AND DISCUSSION

2-Substituted tetrazoles can participate in the formation of homoleptic as well as heteroleptic complexes containing also acetonitrile molecules in the first coordination sphere. Previously, it was shown that reaction of ebtz with zinc(II) perchlorate performed in ethanol leads to formation of a 1D coordination network $[\text{Zn}(\text{ebtz})_3](\text{ClO}_4)_2$, where six tetrazol-2-yl rings form the first coordination sphere of the metal ion.²⁹ SCO phenomena is exhibited by iron(II) complexes possessing $[\text{Fe}(\text{tetrazol-2-yl})_6]^-$ as well as $[\text{Fe}(\text{tetrazol-2-yl})_4(\text{nitrile})_2]$ -type core. Because of that, we have attempted to prepare iron(II) a heteroleptic system containing, in the first coordination sphere, also nitrile molecules beside ebtz. An exchange of ethanol on propionitrile as solvent afforded the $[\text{Fe}(\text{ebtz})_2(\text{C}_2\text{H}_5\text{CN})_2](\text{ClO}_4)_2$ system. Product formation undergoes on slow crystallization from the reaction mixture containing ebtz and iron(II) perchlorate in the molar ratio 2:1. The complex is stable during storage under nitrogen atmosphere; however, crystals are extremely unstable when exposed to air humidity and immediately become cloudy. This reactivity toward water is rather a common feature and is observed in other iron(II) complexes containing coordinated organic nitriles.^{35,36}

Magnetic Susceptibility Measurements. To determine SCO properties the temperature dependent magnetic susceptibility measurements were performed over the 5–300 K range. A $\chi_M T(T)$ dependence was depicted in Figure 1. Upon cooling at a temperature scan rate of 0.1 K/min, in the temperature range 300–117 K, $\chi_M T$ remains almost constant adopting values of 3.52–3.54 $\text{cm}^3 \text{K mol}^{-1}$. Further lowering of temperature involves the abrupt drop in the $\chi_M T$ value with $T_{1/2}^\downarrow = 112$ K. In the temperature range from 116 K ($\gamma_{\text{HS}} = 0.90$) to 108 K ($\gamma_{\text{HS}} = 0.10$, γ_{HS} has been estimated from $[(\chi_M T)_T - (\chi_M T)_{\text{LS}}]/[(\chi_M T)_{\text{HS}} - (\chi_M T)_{\text{LS}}]$, where $(\chi_M T)_T$ represents $\chi_M T$ at temperature T , $(\chi_M T)_{\text{LS}} = 0 \text{ cm}^3 \text{K mol}^{-1}$ and $(\chi_M T)_{\text{HS}} = 3.54 \text{ cm}^3 \text{K mol}^{-1}$) 80% of the HS→LS transition occurs. At 103 K SCO is practically finished, and the $\chi_M T$ value of about 0.12 $\text{cm}^3 \text{K mol}^{-1}$ indicates a practically complete HS→LS transition. After reaching of 5 K, a measurement in the heating mode was performed. 80% of the LS → HS transition ($T_{1/2}^\uparrow = 141$ K) occurs in the range from 137 K ($\gamma_{\text{HS}} = 0.90$) to 145 K ($\gamma_{\text{HS}} = 0.10$). The hysteresis loop ($\Delta T_c = 29$ K) is symmetrical adopting the same width for all $\chi_M T$ values. The course of the spin transition obtained in repeated measurement

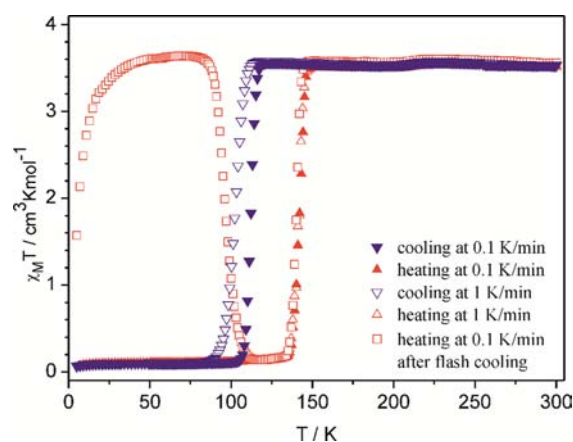


Figure 1. $\chi_M T$ vs T plots for **1** in cooling (blue down triangles) and warming (red up triangles) modes and after flash cooling to 5 K in heating mode (red open squares).

performed at 0.1 K/min was practically the same ($T_{1/2}^\downarrow = 113$ K and $T_{1/2}^\uparrow = 142$ K) as obtained previously at the same temperature scan rate. Cooling of **1** performed at the rate 1 K/min reveals a shift of $T_{1/2}^\downarrow \approx 102$ K to lower temperature values whereas the course of the $\chi_M T$ in the heating mode with the rate 1 K/min is practically the same in relation to measurement performed at 0.1 K. It shows that the investigated complex may be thermally trapped in the HS form.^{37–39} What is more important, such inhibition of SCO may indicate large structural differences between HS and LS forms.⁴⁰ Taking into account that the degree of spin state trapping depends on the cooling rate, we have performed a next experiment depending on flash cooling of the sample.⁴¹ The sample was cooled to 5 K, and the measurement in the heating mode at the scan rate of 0.1 K/min was performed. Upon heating, the $\chi_M T$ increases, because of zero-field splitting of the HS iron(II) ion, reaching a plateau of value 3.6 $\text{cm}^3 \text{K mol}^{-1}$. Further, temperature increase above 80 K involves an abrupt drop of the $\chi_M T$ value. HS→LS relaxation is finished at 110 K. The LS phase obtained this way ($\chi_M T = 0.16 \text{ cm}^3 \text{K mol}^{-1}$) is stable up to about 135 K and then the LS → HS transition with $T_{1/2}^\uparrow = 140$ K starts. Above 145 K the spin transition is finished and $\chi_M T$ is equal to 3.60 $\text{cm}^3 \text{K mol}^{-1}$. A comparison of $\chi_M T$ values, obtained for the quenched phase in the plateau and HS phase above 150 K suggests that flash cooling yields the HS phase practically quantitatively.

Single Crystal X-ray Diffraction Studies. The coordination environment of iron(II) consists of four tetrazole rings forming the basal plane of the octahedron, and two axially coordinated propionitrile molecules (Figure 2). Two ebtz molecules join iron(II) ions, and such linkage is propagated in the a crystallographic direction leading to formation of a 1D chain. Polymeric units, gathered in the (010) plane, are tethered through $\text{C1-H1A}\cdots\text{N1}(1-x, -y, 2-z)$ and $\text{C2-H2B}\cdots\text{N1}(1-x, -y, 2-z)$ weak intermolecular interactions (Figure 3, Supporting Information, Table S1) into 2D supramolecular layers. Coordinated nitrile molecules are directed outward the layer and form in the HS phase very distant contacts $\text{C21-H21B}\cdots\text{N1}(1/2-x, 1/2+y, 3/2-z)$ and $\text{C22-H22A}\cdots\text{N5}(1/2-x, 1/2+y, 3/2-z)$ with tetrazole rings of adjusted supramolecular layers. Consecutive supramolecular layers are separated by perchlorate anions participating in the formation of numerous C–H \cdots O intermolecular contacts (Supporting Information, Table S2, Figures S1 and S2). At 250 K perchlorate anions reveal disorder (30% occupy the

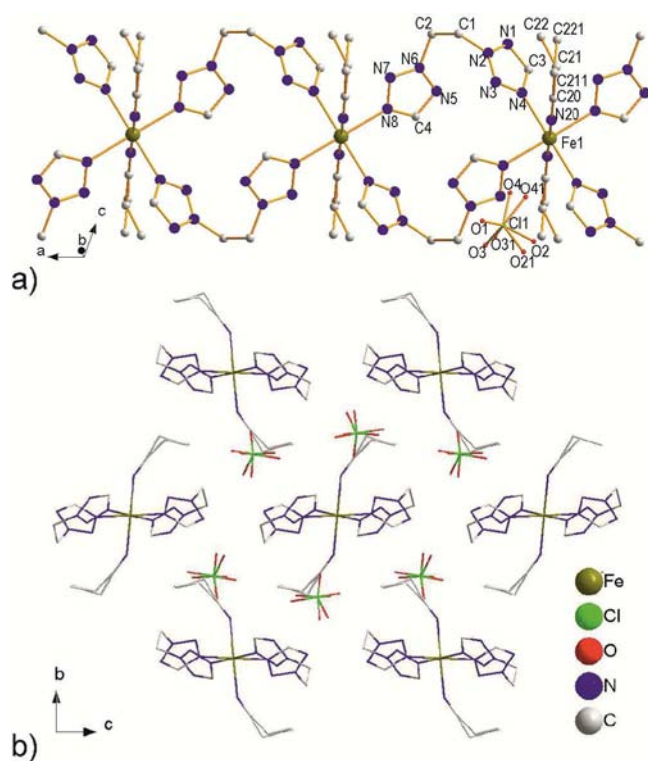


Figure 2. Coordination environment in **1** (a) and bridging fashion of iron(II) ions in 1D chains with labeling scheme of atoms as well as an arrangement of 1D chains along *a* direction (b) (250 K). Hydrogen atoms were omitted for clarity.

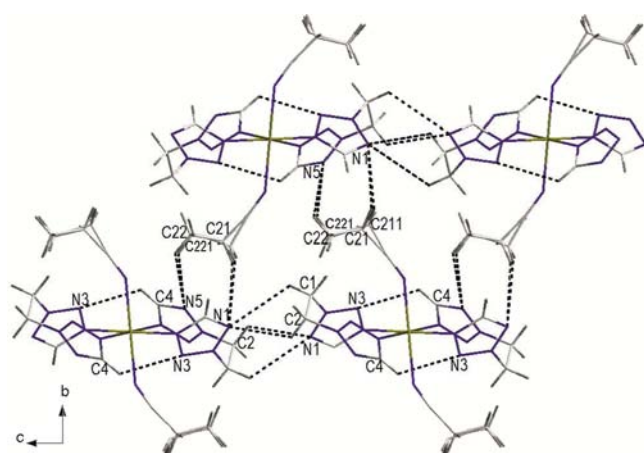


Figure 3. Network of C–H...N contacts established between chains and supramolecular layers. Perchlorate anions were omitted for clarity.

second position), and upon temperature lowering a vanishing of the disorder takes place. At 110 K only 5% of anions adopt the second orientation. The disorder disappears completely when **1** is cooled from 110 to 100 K with the rate 2 K/min. To avoid HS phase quenching, determination of the LS form crystal structure was performed according to results of magnetic studies, cooling crystal from 110 to 80 K with the rate of 0.1 K/min. In the LS form (80 K) perchlorate anions are ordered.

Also in the other 1D network $[\text{Zn}(\text{ebt})_3](\text{ClO}_4)_2$, ebtz molecules act as N4, N4' bridging ligands.²⁹ In Zn(II) and Fe(II) complexes ligand molecules adopt very similar conformation with comparable values of N–C–C–N torsion angle of about 60°. Differences in respective orientations of

azole rings and alkyl spacer result in differentiation of distances between donor atoms (N4–N4' distance is shorter at about 0.7 Å than in **1**). This, as well as differences in respective orientation of coordination octahedrons, result in differentiation of Zn...Zn and Fe...Fe separations. In Zn(II) complex three ebtz molecules join neighboring metal ions at a distance about 1.6 Å shorter than in **1**.

In **1**, at 250 K, the Fe–N4(tetrazol-2-yl), Fe–N8(tetrazol-2-yl), and Fe–N20(C₂H₅CN) distances are equal to 2.179(2), 2.187(2), and 2.146(3) Å, respectively. The N–Fe–N angles are diversified from 87.7(1) to 92.3(1)°. After temperature lowering from 250 to 110 K the Fe–N distances and N–Fe–N angles are virtually the same (Table 2). Also after fast cooling (2 K/min) from 110 to 100 K Fe–N bond lengths remain characteristic for the HS form. At 80 K the Fe–N4, Fe–N8, and Fe–N20 distances are equal to 1.976(3), 1.985(3), and 1.934(3) Å, respectively, indicating a presence of the LS form of iron(II) ions. The FeN₆ chromophore geometry practically remains unchanged after spin transition. Increasing the temperature from 80 to 120 K does not affect the coordination octahedral geometry of the LS form. Increase of temperature from 120 to 160 K is accompanied by the LS→HS transition, and Fe–N bond lengths become comparable to the ones found at 160 K upon cooling.

After HS→LS transition, the intraligand distance between donor atoms N4...N8 insignificantly increases at about 0.01 Å whereas bridged metal ions are separated at 0.21 Å shorter distance in LS than in HS (110 K) phase. For comparison, in 1D SCO systems based on bis(tetrazol-1-yl)ethane-type linkage, reductions of analogous distances at 0.02–0.05 Å and 0.15–0.21 Å takes place, respectively.^{18,19a} So small a change of donor...donor distance in **1** does not result from rigidity of the ebtz molecule. Quite the opposite, the above-mentioned rotation of the tetrazole ring around the N2–C1 bond at about 5° and decrease of the N2–C1–C2–N6 torsion angle is an evidence of the elasticity of the ebtz molecule. An intrachain contact C4–H4A...N3(1–*x*, –*y*, 1–*z*) as well as chain thickness (defined as C1...C2 distance, see Table 2) are reduced at 0.21 and 0.26 Å. Structural transformations of flexible ebtz moieties facilitate further compression of the supramolecular layer and the shortening of chain–chain distances (defined by bridged iron(II) ions) by 0.41 Å. Intermolecular distances between chains of the same layer vary unevenly; the C1–H1A...N1(1–*x*, –*y*, 2–*z*) distance decreases at 0.1 Å whereas C2–H2B...N1(1–*x*, –*y*, 2–*z*) becomes longer at 0.06 Å (Supporting Information, Table S1).

At 250 K, propionitrile molecules, disordered over two positions in the 0.7:0.3 ratio, are coordinated to iron ions in a way that the Fe–N–C(propionitrile) angle is equal to 149.1(3)°. A bent geometry is a really rare feature of coordinated propionitrile and is not a typical for end-bonded nitrile molecules at all. To our best knowledge there are only two known complexes in which the metal–N–C(nitrile) angle is smaller than 150°.⁴² Cooling of the crystal under investigation to 110 K results in gradual decreasing of the Fe–N–C(propionitrile) angle and gradual increasing of the occupancy factor of the major component of the disordered propionitrile molecules. In the temperature range 250–110 K, the ethyl group of the major component of disordered propionitrile molecules is directed parallel to the Fe–N4 bond, and the ethyl group of the minor component (5% in 110 K) adopts a skewed orientation in relation to the Fe–N4 bond. It is worth noticing that at upon fast cooling from 110 to 100 K

Table 2. Selected Bond Lengths (Å), Angles (deg), Torsion Angles (deg), Interatomic Distances (Å), Distances between Chains (Ch, Defined by Bridged Iron(II) Ions) within Supramolecular Layer, Between Plane of Supramolecular Layer (Pl, Defined by Iron(II) Ions Gathered in (010) Plane), and Selected Atoms for 1 in Cooling and Heating (*) Modes and after Fast Cooling (**)

	250(2) K	160(2) K	110(2) K	100(2)K(**)	80(2) K	110(2) K(*)	120(2) K(*)	160(2) K(*)
Fe–N4	2.179(2)	2.176(2)	2.176(2)	2.191(2)	1.976(3)	1.978(3)	1.980(3)	2.172(3)
Fe–N8	2.187(2)	2.185(2)	2.182(2)	2.179(2)	1.985(3)	1.990(3)	1.997(3)	2.183(3)
Fe–N20	2.146(3)	2.148(3)	2.154(2)	2.165(2)	1.934(3)	1.934(3)	1.938(3)	2.146(3)
N4–Fe–N20	92.3(1)	92.3(1)	92.5(1)	92.5(1)	91.6(1)	91.8(1)	91.8(1)	92.2(1)
N8–Fe–N20	91.8(1)	92.0(1)	92.2(1)	92.0(1)	91.6(1)	91.7(1)	91.7(1)	92.1(1)
N4–Fe–N8	91.7(1)	91.8(1)	91.9(1)	92.9(1)	91.7(1)	91.7(1)	91.7(1)	92.0(1)
Fe–N20–C20	149.1(3)	147.3(2)	145.9(2)	145.3(2)	162.9(3)	162.8(3)	162.8(3)	147.0(3)
N20–C20–C21	172.3(7)	175.7(5)	176.4(3)	176.1(2)	174.2(3)	174.4(4)	174.4(4)	176.9(4)
N1–N2–C1–C2	65.3(3)	65.4(3)	65.0(3)	65.9(2)	59.4(3)	59.7(4)	59.8(3)	65.4(4)
N2–C1–C2–N6	63.8(3)	63.6(3)	63.6(3)	63.0(2)	61.4(3)	61.6(3)	61.5(3)	65.6(3)
C1–C2–N6–N5	–74.3(3)	–73.9(3)	–73.3(3)	–73.8(2)	–73.7(4)	–73.8(4)	–73.4(3)	–73.9(4)
N4...N8	5.481(3)	5.461(3)	5.456(3)	5.413(3)	5.472(4)	5.470(4)	5.484(3)	5.465(4)
N2...N6	2.953(3)	2.952(3)	2.952(3)	2.931(2)	2.931(3)	2.928(4)	2.935(3)	2.947(4)
C1...C2 ^a	8.256(4)	8.284(4)	8.299(4)	8.387(4)	8.049(5)	8.042(5)	8.048(5)	8.288(5)
Fe...Fe ^b	8.388(2)	8.364(2)	8.354(2)	8.287(2)	8.144(2)	8.149(2)	8.168(2)	8.363(2)
Fe...Fe ^c	11.616(3)	11.595(3)	11.587(3)	11.692(3)	11.217(3)	11.222(2)	11.242(3)	11.597(3)
Fe...Fe ^d	9.815(2)	9.735(2)	9.688(2)	9.719(2)	9.799(2)	9.802(2)	9.817(2)	9.735(2)
Ch...Ch	11.123	11.111	11.108	11.226	10.690	10.695	10.713	11.111
Pl...C21	4.07(2)	4.10(2)	4.053(4)	4.072(3)	4.187(4)	4.180(4)	4.186(4)	4.090(4)
Pl...N1	0.199(3)	0.196(2)	0.195(2)	0.183(2)	0.435(3)	0.434(3)	0.434(3)	0.197(3)
Pl...N5	0.930(3)	0.913(2)	0.898(2)	0.895(2)	0.966(3)	0.964(3)	0.964(3)	0.912(3)

^aSymmetry operation: $1-x, -y, 1-z$. ^bSymmetry operation: $x+1, y, z$. ^cSymmetry operation: $x, y, z+1$. ^dSymmetry operation: $-0.5-x, 0.5+y, 0.5-z$.

disordering of propionitrile molecule disappears completely and only the component adopting a parallel orientation in relation to the Fe–N4 bond is present. Slow temperature lowering (0.1 K/min) from 110 to 80 K triggers HS→LS transition resulting in a flip-flop of orientation of propionitrile molecule related to a linearization of the Fe–N–C(propionitrile) fragment (from 145.9(2) to 162.9(3)°) and reorientation of the major component to the skewed form (at 80 K propionitrile molecule is ordered) (Figure 4). Return flip-flop, appearance of the bending form of the Fe–N–C(propionitrile) fragment, and appearance of disorder of the propionitrile molecule with its ethyl group of the major component (85%) oriented parallel in

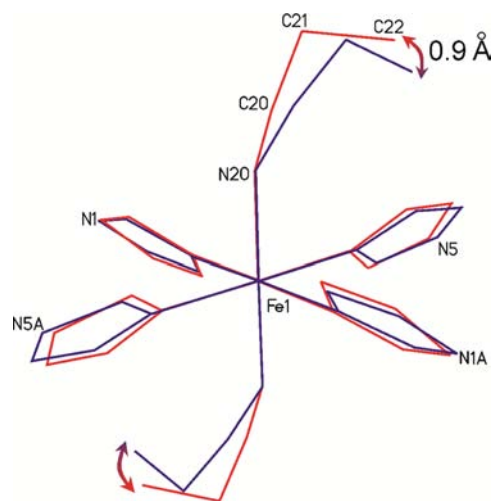


Figure 4. Superpositions of $[\text{Fe}(\text{tetrazol-2-yl})_4(\text{C}_2\text{H}_5\text{CN})_2]$ cores showing different orientations of propionitrile molecules in HS (blue) and LS (red) forms.

relation to the Fe–N4 bond is a result of LS→HS transition during heating from 80 to 160 K.

Typically, in complexes based on coordinated neutral nitrile molecules^{32,33,35} or polynitrile anions⁴³ the geometry of the Fe–N–C(nitrile) fragment is almost linear, and upon HS→LS transition only a slight increase of the Fe–N–C(nitrile) angle (not exceeding 4°) occurs. In iron(II) complexes containing coordinated isothiocyanate anions HS→LS triggers more pronounced changes of the Fe–N–C(S) angle (usually below 10°);^{9,13,38,40,44} however, there are also a few systems in which thermally induced spin transition is associated with larger structural alterations.^{45,46}

In spite of the shortening of the Fe–N bond length during the HS→LS transition, the linearization of the Fe–N–C(propionitrile) fragment causes that distance between supramolecular layers to increase. The flip-flop of orientation of the propionitrile molecule, after slow cooling from 110 to 80 K, results in an increase of the distance between atoms C21 as well as C22 and the supramolecular layer (defined by iron atoms occupying (010) common plane) at 0.13 and 0.15 Å, respectively, and it is combined with a rotation of the tetrazole ring around the N2–C1 bond increasing a distance between nitrogen atom N1 and the supramolecular layer plane at 0.24 Å. In the LS phase C21–H21B...N1($1/2-x, 1/2+y, 3/2-z$) and C22–H22A...N5($1/2-x, 1/2+y, 3/2-z$) intermolecular distances between the supramolecular layers are shorter at 0.13–0.14 Å (see Supporting Information, Table S1 for details). Because of the above-mentioned structural alterations, the separation between supramolecular layers in the LS form is greater at 0.34 Å.

Theoretical considerations of donor–acceptor properties of nitriles show that they exhibit σ , π -donor as well as π -acceptor properties.⁴⁷ Calculations performed for acetonitrile complexes revealed that bending of the metal–N–C(CH₃) fragment

destabilizes $\pi^*(\text{N}\equiv\text{C})$ molecular orbital thus decreasing π -acceptor abilities.⁴⁸ It means that, going from bent to more linear geometry in **1**, the π -back bonding character of nitrile ligand increases, increasing separation (Δ) between t_2 and e orbitals. The observed, slight bending of $\text{N}-\text{C}-\text{C}_2\text{H}_5$ upon going from the HS to the LS structure supports this thesis. Taking into account the above mentioned structural alterations, we assume that the observed linearization of the $\text{Fe}-\text{N}-\text{C}$ (propionitrile) geometry may be related to changes of donor-acceptor properties of nitrile, thus, additionally contributing to the stabilization of the LS form of iron(II).

In dinuclear complexes $[\{\text{Fe}(\text{dpia})(\text{NCS})_2\}_2(\text{bpe})] \cdot n\text{CH}_3\text{OH}$ ($n = 0, 2$) containing coordinated isothiocyanate anions, a strong deviation of the $\text{Fe}-\text{N}-\text{C}$ (isothiocyanate) angle from linearity, which involves decreasing σ , π contributions in ligand field splitting, is pointed to as responsible for transition temperature lowering.⁴⁹

Analysis of the temperature dependency of the interlayer separation ($b/2$) in the HS phase reveals that temperature lowering from 250 to 110 K involves a significant reduction of distance at about 0.16 Å (Figure 5) which is associated with

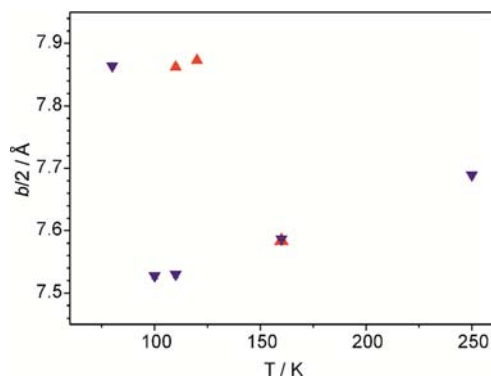


Figure 5. Alteration of interlayer separation ($b/2$) upon cooling (blue down triangles) and heating (red up triangles). Standard deviation $\sigma \leq 0.003$ for b lattice parameter.

decreasing of the $\text{Fe}-\text{N}-\text{C}$ (propionitrile) angle at about 3° (Table 2). The occurrence of a strong compression of the interlayer separation should favor a bent geometry of the $\text{Fe}-\text{N}-\text{C}$ (propionitrile) fragment, thus, contributing to stabilization of the HS form. The HS \rightarrow LS transition involves inversion of these tendencies: a steep increase of interlayer separation and a linearization of the $\text{Fe}-\text{N}-\text{C}$ (propionitrile) fragment takes place. When the crystal is in the LS phase, raising temperature does not affect interlayer separation (Figure 5); thus the linear geometry of the $\text{Fe}-\text{N}-\text{C}$ (propionitrile) fragment is preserved, and the LS form of iron(II) is maintained. Another factor promoting the linear geometry of the $\text{Fe}-\text{N}-\text{C}$ (propionitrile) fragment in the LS phase, might be the shortening of intermolecular contacts $\text{C}21-\text{H}21\text{B}\cdots\text{N}1(1/2-x, 1/2+y, 3/2-z)$ and $\text{C}22-\text{H}22\text{A}\cdots\text{N}5(1/2-x, 1/2+y, 3/2-z)$ and perchlorate anion contacts upon HS \rightarrow LS transition (see Supporting Information). It is worth underlining that contrary to the mononuclear system $[\text{Fe}(\text{H}_4\text{L})_2](\text{ClO}_4)_2 \cdot \text{H}_2\text{O} \cdot 2(\text{CH}_3)_2\text{CO}$ [$\text{H}_4\text{L} = 2,6$ -Bis{5-(2-hydroxyphenyl)-pyrazol-3-yl}pyridine]⁵⁰ in which presence of anion disorder in the HS phase and an absence of anion disorder in the LS phase is pointed to as an origin of bistability, in the HS phase of $[\text{Fe}(\text{ebtz})_2(\text{C}_2\text{H}_5\text{CN})_2](\text{ClO}_4)_2$ lowering of temperature leads to vanishing of anion disordering. We believe that

the molecular-level coupling between temperature-dependent interlayer distances and distinctly different geometries of $\text{Fe}-\text{N}-\text{C}$ (propionitrile) fragments in HS and LS forms is fundamental for the occurrence of bistability observed in the studied system.

It is worth mentioning, that similar structural processes are observed in the coordination network $[\text{Fe}(\text{btr})_2(\text{NCS})_2] \cdot \text{H}_2\text{O}$ ($\text{btr} = 4,4'$ -bis(1,2,4-triazole)) which exhibits layered architecture as well.⁴⁶ Also in this complex, the HS \rightarrow LS transition is associated with reorientation of the NCS group leading to a more linear geometry of the $\text{Fe}-\text{N}-\text{C}(\text{S})$ fragment in the LS phase and increase of the separation between the 2D polymeric layers. And also in this case SCO is very abrupt and accompanied by a hysteresis loop (of width 21 K).

SUMMARY

In the crystal of $[\text{Fe}(\text{ebtz})_2(\text{C}_2\text{H}_5\text{CN})_2](\text{ClO}_4)_2$ 1D chains are tethered through weak $\text{C}-\text{H}\cdots\text{N}$ intermolecular interactions into supramolecular layers in such a way that axially coordinated propionitrile molecules are directed outward to the layers. The unusual feature is a bent geometry of the $\text{Fe}-\text{N}-\text{C}$ (propionitrile) fragment in the HS form of the complex and the ability of the coordinated propionitrile molecule to reorient in relation to the coordination octahedron. The HS \rightarrow LS transition switches the orientation of the propionitrile molecule which leads to a linearization of the $\text{Fe}-\text{N}-\text{C}(\text{C}_2\text{H}_5)$ fragment and increase in the separation between supramolecular layers. In the heating mode, in the absence of changes to interlayer distances, the more linear form of $\text{Fe}-\text{N}-\text{C}(\text{C}_2\text{H}_5)$ is favored, which contributes to further stabilization of the LS phase. Thus, a combination of molecular and lattice based effects results in bistability of the complex.

Recently we have shown how subtle changes of intermolecular interactions established between polymeric units are crucial for the occurrence of thermally induced spin transition in the 2D coordination polymer $[\text{Fe}(\text{bbtr})_3](\text{ClO}_4)_2$.^{25b} In the current paper, we have demonstrated that significant structural alterations coupled through intermolecular interactions represent a key factor for SCO properties. Additionally, we have proved that application of elastic bridging ligands does not preclude construction of highly cooperative SCO materials revealing a wide thermal hysteresis loop.

ASSOCIATED CONTENT

Supporting Information

Tables S1 and S2, Figures S1 and S2, X-ray crystallographic files in CIF format. This material is available free of charge via the Internet at <http://pubs.acs.org>.

AUTHOR INFORMATION

Corresponding Author

*E-mail: robert.bronisz@chem.uni.wroc.pl

Notes

The authors declare no competing financial interest.

ACKNOWLEDGMENTS

We thank the Ministry of Science and Higher Education for their financial support of this research.

REFERENCES

- (a) Gütllich, P.; Goodwin, H. A. *Top. Curr. Chem.* **2004**, 233, 1–47. (b) Gütllich, P.; Garcia, Y.; Goodwin, H. A. *Chem. Soc. Rev.* **2000**,

- 29, 419–427. (c) Gütlich, P.; Hauser, A.; Spiering, H. *Angew. Chem., Int. Ed. Engl.* **1994**, *33*, 2024–2054.
- (2) Ksenofontov, V.; Gaspar, A. P.; Gütlich, P. *Top. Curr. Chem.* **2004**, *235*, 23–64.
- (3) Bousseksou, A.; Varret, F.; Goiran, M.; Boukheddaden, K.; Tuchagues, J. P. *Top. Curr. Chem.* **2004**, *235*, 65–84.
- (4) (a) Decurtins, S.; Gütlich, P.; Köhler, C. P.; Spiering, H.; Hauser, A. *Chem. Phys. Lett.* **1984**, *105*, 1–4. (b) Hauser, A. *Top. Curr. Chem.* **2004**, *234*, 155–198.
- (5) (a) Bousseksou, A.; Molnar, G.; Demont, P.; Menegotto, J. J. *Mater. Chem.* **2003**, *13*, 2069–2071. (b) Bonhommeau, S.; Guillon, T.; Lawson Daku, L. M.; Demont, P.; Costa, J. S.; Letard, J.-F.; Molnar, G.; Bousseksou, A. *Angew. Chem., Int. Ed.* **2006**, *45*, 1625–1629.
- (6) (a) Letard, J.-F.; Guionneau, P.; Goux-Capes, L. *Top. Curr. Chem.* **2004**, *235*, 221–249. (b) Bousseksou, A.; Molnar, G.; Salmon, L.; Nicolazzi, W. *Chem. Soc. Rev.* **2011**, *40*, 3313–3335. (c) Bousseksou, A.; Molnar, G.; Matouzenko, G. *Eur. J. Inorg. Chem.* **2004**, 4353–4369.
- (7) Kahn, O.; Launay, J.-P. *Chemtronics* **1988**, *3*, 140–151.
- (8) (a) Spiering, H.; Boukheddaden, K.; Linares, J.; Varret, F. *Phys. Rev. B* **2004**, *70*, 184106. (b) Spiering, H. *Top. Curr. Chem.* **2004**, *235*, 171–195.
- (9) Takahashi, K.; Kawakami, T.; Gu, Z.-Z.; Einaga, Y.; Fujishima, A.; Sato, O. *Chem. Commun.* **2003**, 2374–2375.
- (10) (a) Dorbes, S.; Valade, L.; Real, J. A.; Faulmann, C. *Chem. Commun.* **2005**, 69–71. (b) Weber, B.; Bauer, W.; Obel, J. *Angew. Chem. Int. Ed.* **2008**, *47*, 10098–10101. (c) Letard, J. F.; Guionneau, P.; Codjovi, E.; Lavastre, O.; Bravic, C.; Chasseau, D.; Kahn, O. *J. Am. Chem. Soc.* **1997**, *119*, 10861–10862. (d) Zhong, Z. J.; Tao, J.; Yu, Z.; Dun, C.; Liu, Y.; You, X. *J. Chem. Soc., Dalton Trans.* **1998**, 327–328. (e) Halcrow, M. A. *Chem. Soc. Rev.* **2011**, *40*, 4119–4142.
- (11) Reger, D. L.; Little, C. A.; Young, V. G.; Maren, P. *Inorg. Chem.* **2001**, *40*, 2870–2874.
- (12) (a) Spiering, H.; Kohlhaas, T.; Romstedt, H.; Hauser, A.; Bruns-Yilmaz, C.; Kusz, J.; Gütlich, P. *Coord. Chem. Rev.* **1999**, *190*–192, 629–647. (b) Chernyshov, D.; Hostettler, M.; Tornroos, K. W.; Bürgi, H.-B. *Angew. Chem. Int. Ed.* **2003**, *42*, 3825–3830. (c) Kusz, J.; Schollmeyer, D.; Spiering, H.; Gütlich, P. *J. Appl. Crystallogr.* **2005**, *38*, 528–536. (d) W. Tornroos, K.; Hostettler, M.; Chernyshov, D.; Vangdal, B.; Bürgi, H.-B. *Chem.—Eur. J.* **2006**, *12*, 6207–6215. (e) Kusz, J. *Solid State Phenom.* **2007**, *130*, 199–202. (f) Brefuel, N.; Watanabe, H.; Toupet, L.; Come, J.; Matsumoto, N.; Collet, E.; Tanaka, K.; Tuchagues, J.-P. *Angew. Chem., Int. Ed.* **2009**, *48*, 9304–9307. (g) Hostettler, M.; Tornroos, K. W.; Chernyshov, D.; Vangdal, B.; Bürgi, H.-B. *Angew. Chem., Int. Ed.* **2004**, *43*, 4589–4594. (h) Boinnard, D.; Bousseksou, A.; Dworkin, A.; Savariault, J.-M.; Varret, F.; Tuchagues, J.-P. *Inorg. Chem.* **1994**, *33*, 271–281. (i) Griffin, M.; Shakespeare, S.; Shepherd, H. J.; Harding, C. J.; Letard, J. F.; Desplanches, A.; Goeta, E.; Howard, J. A. K.; Powell, A. K.; Mereacre, V.; Garcia, Y.; Naik, A. D.; Muller-Bunz, H.; Morgan, G. G. *Angew. Chem., Int. Ed.* **2011**, *50*, 896–900.
- (13) Bonnet, S.; Siegler, M. A.; Costa, J. S.; Molnar, G.; Bousseksou, A.; Spek, A. L.; Gamez, P.; Reedijk, J. *Chem. Commun.* **2008**, 5619–5621.
- (14) Kahn, O.; Codjovi, E.; Garcia, Y.; van Koningsbruggen, P. J.; Lapayoudi, R.; Sommier, L. *ACS Symp. Ser.* **1996**, *644*, 298–310.
- (15) Real, J. A.; Andres, E.; Munoz, C. M.; Julve, M.; Granier, T.; Bousseksou, A.; Varret, F. *Science* **1995**, *268*, 265–267.
- (16) (a) Moulton, B.; Zaworotko, M. J. *Chem. Rev.* **2001**, *101*, 1629–1658. (b) Kitagawa, S.; Kitaura, R.; Noro, S.-I. *Angew. Chem., Int. Ed.* **2004**, *43*, 2334–2375.
- (17) (a) Absmeier, A.; Bartel, M.; Carbonera, C.; Jameson, G. N. L.; Werner, F.; Reissner, M.; Caneschi, A.; Létard, J.-F.; Linert, W. *Eur. J. Inorg. Chem.* **2007**, 3047–3054. (b) Absmeier, A.; Bartel, M.; Carbonera, C.; Jameson, G. N. L.; Weinberger, P.; Caneschi, A.; Mereiter, K.; Létard, J.-F.; Linert, W. *Chem.—Eur. J.* **2006**, *12*, 2235–2243.
- (18) (a) Schweifer, J.; Weinberger, P.; Mereiter, K.; Boca, M.; Reichl, C.; Wiesinger, G.; Hilscher, G.; van Koningsbruggen, P. J.; Kooijman, H.; Grunert, M.; Linert, W. *Inorg. Chim. Acta* **2002**, *339*, 297–306.
- (b) van Koningsbruggen, P. J.; Garcia, Y.; Fournes, L.; Kooijman, H.; Spek, A. L.; Haasnoot, J. G.; Moscovici, J.; Provost, K.; Michalowicz, A.; Renz, F.; Gütlich, P. *Inorg. Chem.* **2000**, *39*, 1891–1900.
- (19) (a) Quesada, M.; Kooijman, H.; Gamez, P.; Costa, J. S.; van Koningsbruggen, P. J.; Weinberger, P.; Reissner, M.; Spek, A. L.; Haasnoot, J. G.; Reedijk, J. *Dalton Trans.* **2007**, 5434–5440. (b) Quesada, M.; Prins, F.; Bill, E.; Kooijman, H.; Gamez, P.; Roubeau, O.; Spek, A. L.; Haasnoot, J. G.; Reedijk, J. *Chem.—Eur. J.* **2008**, *14*, 8486–8499.
- (20) Quesada, M.; Prins, F.; Roubeau, O.; Gamez, P.; Teat, S. J.; van Koningsbruggen, P. J.; Haasnoot, J. G.; Reedijk, J. *Inorg. Chim. Acta* **2007**, *360*, 3787–3796.
- (21) (a) Grunert, C. M.; Schweifer, J.; Weinberger, P.; Linert, W.; Mereiter, K.; Hilscher, G.; Mueller, M.; Wiesinger, G.; van Koningsbruggen, P. J. *Inorg. Chem.* **2004**, *43*, 155–165. (b) Bartel, M.; Absmeier, A.; Jameson, G. N. L.; Werner, F.; Kato, K.; Takata, M.; Boca, R.; Hasegawa, M.; Mereiter, K.; Caneschi, A.; Linert, W. *Inorg. Chem.* **2007**, *46*, 4220–4229. (c) van Koningsbruggen, P. J.; Garcia, Y.; Kooijman, H.; Spek, A. L.; Haasnoot, J. G.; Kahn, O.; Linares, J.; Codjovi, E.; Varret, F. *J. Chem. Soc., Dalton Trans.* **2001**, 466–471. (d) Jameson, G. N. L.; Werner, F.; Bartel, M.; Absmeier, A.; Reissner, M.; Kitchen, J. A.; Brooker, S.; Caneschi, A.; Carbonera, C.; Létard, J.-F.; Linert, W. *Eur. J. Inorg. Chem.* **2009**, 3948–3959.
- (22) (a) Grunert, C. M.; Weinberger, P.; Schweifer, J.; Hampel, C.; Stassen, A. F.; Mereiter, K.; Linert, W. *J. Mol. Struct.* **2005**, *733*, 41–52. (b) Muttenthaler, M.; Bartel, M.; Weinberger, P.; Hilscher, G.; Linert, W. *J. Mol. Struct.* **2005**, *741*, 159–1692.
- (23) (a) Bronisz, R.; Ciunik, Z.; Drabent, K.; Rudolf, M. F. *Conf. Proc., ICAME-95* **1996**, *50*, 15–18. (b) Bialońska, A.; Bronisz, R.; Rudolf, M. F.; Weselski, M. *Inorg. Chem.* **2012**, *51*, 237–245.
- (24) Halcrow, M. A. *Polyhedron* **2007**, *26*, 3523–3576, and references cited therein.
- (25) (a) Bronisz, R. *Inorg. Chem.* **2005**, *44*, 4463–4465. (b) Kusz, J.; Bronisz, R.; Zubko, M.; Bednarek, G. *Chem.—Eur. J.* **2011**, *17*, 6807–6820. (c) Bialońska, A.; Bronisz, R.; Kusz, J.; Weselski, M.; Zubko, M. *Eur. J. Inorg. Chem.* DOI: 10.1002/ejic.201200645; (d) Bialońska, A.; Bronisz, R.; Kusz, J.; Zubko, M. *Eur. J. Inorg. Chem.* DOI: 10.1002/ejic.201200960.
- (26) Aromi, G.; Barrios, L. A.; Roubeau, O.; Gamez, P. *Coord. Chem. Rev.* **2011**, *255*, 485–546.
- (27) Moliner, N.; Munoz, M. C.; Letard, S.; Solans, X.; Menendez, N.; Goujon, A.; Varret, F.; Real, J. A. *Inorg. Chem.* **2000**, *39*, 5390–5393.
- (28) (a) Murray, K. S. *Eur. J. Inorg. Chem.* **2008**, 3101–3121. (b) Bauer, W.; Dirlu, M. M.; Garcia, Y.; Weber, B. *CrystEngComm* **2012**, *14*, 1223–1231.
- (29) Bronisz, R. *Inorg. Chim. Acta* **2002**, *340*, 215–220.
- (30) (a) Bronisz, R. *Eur. J. Inorg. Chem.* **2004**, 3688–3695. (b) Bronisz, R. *Inorg. Chim. Acta* **2004**, *357*, 396–404.
- (31) Bronisz, R. *Inorg. Chem.* **2007**, *46*, 6733–6739.
- (32) Bialońska, A.; Bronisz, R.; Weselski, M. *Inorg. Chem.* **2008**, *47*, 4436–4438.
- (33) Bialońska, A.; Bronisz, R. *Inorg. Chem.* **2010**, *49*, 4534–4542.
- (34) Sheldrick, G. M. *Acta Crystallogr., Sect. A* **2008**, *64*, 112–122.
- (35) Chainok, K.; Neville, S. M.; Moubaraki, B.; Battena, S. R.; Murray, K. S.; Forsyth, C. M.; Cashin, J. D. *Dalton Trans.* **2010**, *39*, 10900–10909.
- (36) (a) Quesada, M.; de la Peña-O’Shea, V. A.; Aromi, G.; Geremia, S.; Massera, C.; Roubeau, O.; Gamez, P.; Reedijk, J. *Adv. Mater.* **2007**, *19*, 1397–1402. (b) Bialońska, A.; Bronisz, R.; Darowska, K.; Drabent, K.; Kusz, J.; Siczek, M.; Weselski, M.; Zubko, M.; Ożarowski, A. *Inorg. Chem.* **2010**, *49*, 11267–11269.
- (37) (a) Buchen, Th.; Gütlich, P.; Goodwin, H. A. *Inorg. Chem.* **1994**, *33*, 4573–4576. (b) Buchen, Th.; Gütlich, P.; Sugiyarto, K. H.; Goodwin, H. A. *Chem.—Eur. J.* **1996**, *9*, 1134–1138. (c) Yamada, M.; Hagiwara, H.; Torigoe, H.; Matsumoto, N.; Kojima, M.; Dahan, F.; Tuchagues, J. P.; Re, N.; Iijima, S. *Chem.—Eur. J.* **2006**, *12*, 4536–4549.

- (38) Neville, S. M.; Leita, B. A.; Halder, G. J.; Kepert, C. J.; Moubaraki, B.; Letard, J.-F.; Murray, K. S. *Chem.—Eur. J.* **2008**, *14*, 10123–10133.
- (39) Money, V. A.; Carbonera, C.; Elhaik, J.; Halcrow, M. A.; Howard, J. A. K.; Letard, J.-F. *Chem.—Eur. J.* **2007**, *13*, 5503–5514.
- (40) Halder, G. J.; Chapman, K. W.; Neville, S. M.; Moubaraki, B.; Murray, K. S.; Letard, J.-F.; Kepert, C. J. *J. Am. Chem. Soc.* **2008**, *130*, 17552–17562.
- (41) Marchivie, M.; Guionneau, P.; Letard, J.-F.; Chasseau, D.; Howard, J. A. K. *J. Phys. Chem. Solids* **2004**, *65*, 17–23.
- (42) (a) Ibrahim, A. A.; Blachnik, R.; Reuter, H.; Stumpf, K. Z. *Kristallogr.-New Cryst. Struct.* **1999**, *214*, 119–120. (b) Zang, S.-Q.; Cheng, P.-S.; Mak, T. C. W. *CrystEngComm* **2009**, *11*, 1061–1067.
- (43) Dupouy, G.; Marchivie, M.; Triki, S.; Sala-Pala, J.; Salaun, J.-Y.; Gomez-Garcia, C. J.; Guionneau, P. *Inorg.Chem.* **2008**, *47*, 8921–8931.
- (44) (a) Verat, A. Yu.; Ould-Moussa, N.; Jeanneau, E.; Le Guennic, B.; Bousseksou, A.; Borshch, S. A.; Matouzenko, G. S. *Chem.—Eur. J.* **2009**, *15*, 10070–10082. (b) Letard, J.-F.; Kollmansberger, M.; Carbonera, C.; Marchivie, M.; Guionneau, P. *C. R. Chim.* **2008**, *11*, 1155–1165. (c) Galet, A.; Gaspar, A. B.; Munoz, M. C.; Levchenko, G. J.; Real, A. *Inorg. Chem.* **2006**, *45*, 9670–9679. (d) Klingele, J.; Kaase, D.; Klingele, M. H.; Lach, J.; Demeshko, S. *Dalton Trans.* **2010**, *39*, 1689–1691. (e) Gaspar, A. B.; Ksenofontov, V.; Reiman, S.; Gutlich, P.; Thompson, A. L.; Goeta, A. E.; Munoz, M. C.; Real, J. A. *Chem.—Eur. J.* **2006**, *12*, 9289–9298. (f) Glijer, D.; Hebert, J.; Trzop, E.; Collet, E.; Toupet, L.; Cailleau, H.; Matouzenko, G. S.; Lazar, H. Z.; Letard, J. F.; Koshihara, S.; Cointe, M. B.-L. *Phys. Rev. B: Condens. Matter* **2008**, *78*, 134112. (g) Kaiba, A.; Shepherd, H. J.; Fedaoui, D.; Rosa, P.; Goeta, A. E.; Rebbani, N.; Letard, J. F.; Guionneau, P. *Dalton Trans.* **2010**, *39*, 2910–2918. (h) Quesada, M.; Monrabal, M.; Aromi, G.; de la Pena-O’Shea, V. A.; Gich, M.; Molins, E.; Roubeau, O.; Teat, S. J.; MacLean, E. J.; Gamez, P.; Reedijk, J. J. *Mater. Chem.* **2006**, *16*, 2669–2676. (i) Neville, S. M.; Halder, G. J.; Chapman, K. W.; Duriska, M. B.; Southon, P. D.; Cashion, J. D.; Letard, J.-F.; Moubaraki, B.; Murray, K. S.; Kepert, C. J. *J. Am. Chem. Soc.* **2008**, *130*, 2869–2876. (j) Sheu, C.-F.; Chen, S.-M.; Wang, S.-C.; Lee, G.-H.; Liu, Y.-H.; Wang, Y. *Chem. Commun.* **2009**, 7512–7514. (k) Shuku, Y.; Suizu, R.; Awaga, K.; Sato, O. *CrystEngComm* **2009**, *11*, 2065–2068. (l) Sheu, C.-F.; Chen, K.; Chen, S.-M.; Wen, Y.-S.; Lee, G.-H.; Chen, J.-M.; Lee, J.-F.; Cheng, B.-M.; Sheu, H.-S.; Yasuda, N.; Ozawa, Y.; Toriumi, K.; Wang, Y. *Chem.—Eur. J.* **2009**, *15*, 2384–2393. (m) Guionneau, P.; Letard, J.-F.; Yufit, D. S.; Chasseau, D.; Bravic, G.; Goeta, A. E.; Howard, J. A. K.; Kahn, O. *J. Mater. Chem.* **1999**, *9*, 985–994. (n) Gallois, B.; Real, J.-A.; Hauw, C.; Zarembowitch, J. *Inorg. Chem.* **1990**, *29*, 1152–1158. (o) Granier, T.; Gallois, B.; Gaultier, J.; Real, J.-A.; Zarembowitch, J. *Inorg. Chem.* **1993**, *32*, 5305–5312. (p) Real, J. A.; Munoz, M. C.; Andres, E.; Granier, T.; Gallois, B. *Inorg. Chem.* **1994**, *33*, 3587–3594.
- (45) (a) Amoore, J. J. M.; Kepert, C. J.; Cashion, J. D.; Moubaraki, B.; Neville, S. M.; Murray, K. S. *Chem.—Eur. J.* **2006**, *12*, 8220–8227. (b) Brefuel, N.; Shova, S.; Lipkowski, J.; Tuchagues, J.-P. *Chem. Mater.* **2006**, *18*, 5467–5479. (c) Neville, S. M.; Leita, B. A.; Offermann, D. A.; Duriska, M. B.; Moubaraki, B.; Chapman, K. W.; Halder, G. J.; Murray, K. S. *Eur. J. Inorg. Chem.* **2007**, 1073–1085. (d) Kusz, J.; Zubko, M.; Fitch, A.; Gütllich, P. *Z. Kristallogr.* **2011**, 576–584.
- (46) (a) Vreugdenhil, W.; van Diemen, J. H.; de Graaf, R. A. G.; Haasnoot, J. G.; Reedijk, J.; van der Kraan, A. M.; Kahn, O.; Zarembowitch, J. *Polyhedron* **1990**, *9*, 2971–2979. (b) Pillet, S.; Hubsch, J.; Lecomte, C. *Eur. Phys. J. B* **2004**, *38*, 541–552. (c) Legrand, V.; Pillet, S.; Carbonera, C.; Souhassou, M.; Létard, J.-F.; Guionneau, P.; Lecomte, C. *Eur. J. Inorg. Chem.* **2007**, 5693–5706.
- (47) Kuznetsov, M. L. *Russ. Chem. Rev.* **2002**, *71*, 265–282.
- (48) Howell, J. A.; Saillard, J.-Y.; Le Beuze, A.; Jaouen, G. *J. Chem. Soc. Dalton Trans.* **1982**, 2533–2537.
- (49) (a) Matouzenko, G. S.; Jeanneau, E.; Verat, A. Yu.; Bousseksou, A. *Dalton Trans.* **2011**, *40*, 9608–9618. (b) Matouzenko, G. S.; Jeanneau, E.; Verat, A. Yu.; de Gaetano, Y. *Eur. J. Inorg. Chem.* **2012**, 969–977.
- (50) Craig, G. A.; Costa, J. S.; Roubeau, O.; Teat, S. J.; Aromi, G. *Chem.—Eur. J.* **2011**, *17*, 3120–3127.